CRACK CLOSURE AND MICROSTRUCTURALLY SHORT FATIGUE CRACK GROWTH RATES

Ken Gall and Huseyin Sehitoglu[1]
Department of Mechanical and Industrial Engineering
University of Illinois, Urbana IL 61801

ABSTRACT

Previous research efforts modeling fatigue crack closure have assumed that the material surrounding the crack tip behaves isotropically. The current model implements a double slip geometry to simulate fatigue cracks traversing through the microstructure using finite elements. By varying the crystallographic orientation of the slip systems in the model, with respect to the crack growth direction, fatigue crack closure levels, $S_{open} / S_{\max}$, were found to vary in the range 0.02 to 0.35. Corresponding to this variation, a nonlinear crack growth law was used to estimate expected variations in crack growth rates for microstructurally short fatigue cracks when they grow through grains with different orientations. The resulting predictions for $\frac{da}{dN}$ variations span the range $1.5 \leq \frac{da}{dN}(\max) / \frac{da}{dN}(\min) \leq 60$, corresponding to a change in the crack growth exponent, m, from 1 to 10.

KEYWORDS

Crack closure, short cracks, variable growth rates, microstructure, finite element analysis.

INTRODUCTION

One important area of experimental research on fatigue crack growth considered long fatigue crack growth in single crystals (McEvily et al. 1963, Neumann 1969, Pelloux 1969). An important finding of these early experiments was that the crack growth rates varied as the orientation of the crystal, with respect to the growth direction, was changed (Pelloux 1969). The growth variability caused by different crystallographic orientations was also noted in the study of microstructurally short fatigue cracks (MSC's) (Morris and James 1983, Chan 1987, Larson et al. 1988, Ritchie et al. 1988, Tanaka 1984 and 1989). The orientation of individual grains, with respect to the crack growth direction, may favor an increase, decrease, or even an arrest of the crack growth rate. Since the crack growth rates of short cracks can dramatically influence fatigue lives, it is imperative that any crack growth modeling reflects the underlying microstructure. Table 1 summarizes some short crack growth rate variability which has been experimentally observed for several different materials. The investigators name, material grain size, and crack length range are also given in table 1. The crack length ranges are the initial and final lengths of the growing fatigue cracks being studied. The $\frac{da}{dN}(\max) / \frac{da}{dN}(\min)$ values are calculated by exclusively considering cracks that continued to grow until failure. From table 1 it is clear that the growth rate variability is larger when the growth increment is larger than the average grain size.

---

[1] Graduate Research Assistant and Professor, respectively.

To quantify the variability is MSC growth rates, Morris and his coworkers (1977 and 1983) used changes in closure stress levels as a crack traversed through the microstructure. They concluded that as a crack approaches a grain boundary, the closure stresses decrease while the fatigue crack growth rates increase. However, they did not study the effect of many different crystallographic orientations on the growth rates. To better quantify the variability, a finite element analysis, with plastic flow allowed exclusively along two specified microscopic crystallographic planes, is used to model the MSC's. When the crack tip plastic zone size is close to the average grain size, crack growth rates are influenced by the orientation of the crack tip grains. In engineering applications this may occur when a short crack grows within a grain, a long crack grows through a large or single grain microstructure, or when any crack is driven at near threshold stress intensity amplitudes. This study will focus on mode I through thickness cracks in single crystals, and the crack growth rate variability caused by different orientations. By varying the directions of the microscopic slip traces, the effect of different crystallographic orientations on plasticity induced fatigue crack closure levels will be quantified. Then, using a power law fatigue crack growth law along with expected variations in closure stresses, differences in crack growth rates will be predicted. As a first approximation, the effect of neighboring grains will not be considered.

FINITE ELEMENT MODEL

A detailed description of the time independent elastic-plastic 'double slip' F.E.M. has been previously presented and discussed (Gall, Sehitoglu, and Kadioglu 1996-I, 1996-II, 1996-III). The plastic constitutive relationship is based on a plane strain double slip plane model proposed by Asaro and coworkers (1978, 1983, 1991) (figure 1a). The double slip model is chosen since experimental evidence indicates the exclusive activation of two slip systems in fatigue crack growth (Neumann 1969, Pelloux 1969). Plastic deformation occurs along two slip planes which are characterized by unit vectors (s_1,m_1) and (s_2,m_2). The vectors are trigonometric functions of the two angles in figure 1a. The angle between either slip plane and the Y-direction (loading direction) of the crystal is called Θ, and the orientation of the crystal with respect to the X-direction (crack growth direction) is called ϕ. Both slip directions and slip plane normals lie in the plane of the drawing. This model has been successfully used to model the tensile deformation of both BCC and FCC crystals (Asaro 1978) and later to study single crystal cracked bodies (Rice et al. 1990).

The finite element mesh used here is the center cracked panel (CCP) with crack initiation at an elliptical notch (Gall et al 1996-I). The fine mesh region has a $\Delta a/W$ value of .0013 where W is specimen width. In this analysis, the crack is grown out of the notch stress field, allowing one to approximate the notch specimen as an ideal center cracked panel. Crack advance is accomplished by releasing crack tip nodes at the maximum load in each cycle. This creates an effective crack growth rate of Δa mesh units per cycle. The changing crack line boundary conditions are handled by a series of truss elements (Sehitoglu and McClung 1989 1,2). The far field loads are applied incrementally, with 50 load increments per reversal (half cycle). The simulation is conducted for a total of 20 cycles (2000 total increments) under R=0 loading. All of the results in this paper were created at the far field stress ratio $S_{max}/S_y = 0.6$. S_y is the uniaxial yield stress of an individual double slip Θ and ϕ combination. It should be noted that S_y varies as Θ and ϕ are changed (Gall et al. 1996-I). Since different double slip orientations are studied at the same S_{max}/S_y level (0.6), various far field loads are applied for different double slip cases. Each simulation runs for approximately .7 hours on the NCSA Power Challenge Supercomputer, Urbana, Illinois.

VARIATIONS IN CRACK CLOSURE LEVELS

To obtain the steady state crack closure levels as a function of different microscopic slip configurations (ϕ and Θ), the angle ϕ was varied while keeping the angle between the slip planes, Θ, constant at 30°. Conversely, a different study maintained ϕ at 0° while varying Θ (Gall et al. 1996-I). Varying ϕ had a pronounced effect on the steady state plasticity induced crack closure levels of the fatigue crack. Figure 1b displays the variation of S_{open}/S_{max} over the ϕ angle range 0 to 90°. Due to the symmetry of the model, the angle ranges 90°-180°, 180°-270°, and 270°-360° take the same shape as Figure 1b. The opening behavior has two distinct regions. One region has relatively high opening levels, $S_{open}/S_{max} = 0.35$, while the other region has extremely low levels, $S_{open}/S_{max} = 0.02$. The model produced similar closure level variations when ϕ was kept fixed and Θ was varied (Gall et al. 1996-I).

In previous research efforts, many researchers have concluded that microstructurally short the cracks do not develop significant levels of crack closure due to their relatively short crack wake. This may be the case when the cracks are *extremely* small $a < 10$ μm, however, the cracks in this study are as long as 400 μm. To demonstrate how closure develops in these MSC's, the crack tip stress-strain behavior will be examined. Since plane strain plasticity induced closure is caused by material transfer to crack surfaces from the crack growth direction (Sehitoglu and Wei 1991), one can compare the stress-strain (σ-ε) response of the crack tip in the X and Y directions. To do this, the stress-strain response of an element (# 276) initially far from the crack tip, which is being approached by the crack tip, is monitored throughout the loading history (figures 2a and 2b). The crack starts at the element which is furthest to the left on figure 2a, and it progresses incrementally along the bottom of the fine mesh region. At the final loading cycle the crack tip is located at element 276, hence the gauss point in this element closest to the crack tip is called the 'material point' (figure 2a). In Figure 2b plots of the stress-strain response for the case where $\phi = 30°$ and $\Theta = 30°$ are shown. As the crack approaches element 276, this element accumulates *negative* residual plastic strains in the x-direction. This confirms that the mechanism of material transfer to the crack surfaces is the same in the case of double slip or isotropic material behavior. A final measure of residual strains can be calculated by taking the distance along the horizontal axis between the origin and the intersection of the final reversal. The final strain values are nearly equal indicating that the cumulative residual compressive strains in the x-direction directly contribute to the cumulative residual tensile strains in the y-direction and vice versa. The difference in the magnitude of these residual plastic strains for different crystallographic orientations is one reason for crack opening levels to differ greatly among orientations.

Variations in opening levels for cracks with plastic zones confined to single grains have been experimentally observed by Morris (Morris 1977, 1980). The crack opening stresses in his studies were found to vary from $S_{open} / S_{max} = .2$ to $S_{open} / S_{max} = .75$ for cracks with plastic zones confined to one grain. The values found in this F.E.M. study are smaller (.05 to .35). The difference can be attributed to the plane strain conditions studied here, instead of the plane stress conditions seen by surface cracks. Additionally, the model here ignores the roughness induced crack closure contribution.

SHORT CRACK GROWTH RATE PREDICTIONS

Growth rate variability for microstructurally short fatigue cracks is caused by changes in the crack tip driving forces as short cracks traverse through grains with different crystallographic orientations. One way to quantify the variability in MSC growth rates is through the effective stress intensity range, ΔK_{eff}. By using a modified crack growth law,

$$\frac{da}{dN} = C(\Delta K_{eff})^m \quad (1)$$

along with changes in the closure stress values, one can set bounds on expected changes in short fatigue crack growth rates. To calculate the adjusted fatigue crack growth rate incrementally along the entire short crack growth curve would be very difficult since the point by point transient closure stress levels are not known during the growth period. However, one can determine upper and lower bounds on the variability of short fatigue crack growth rates using the maximum and minimum crack closure levels. The maximum growth rate will occur when the closure stresses are extremely low, while the minimum growth rate will occur when the closure levels are extremely high. Using the definition of effective stress intensity range, and substituting in the maximum (S_{open}/S_{max} = 0.35) and minimum (S_{open}/S_{max} = 0.02) opening levels, over all possible crystallographic orientations, one obtains the following:

$$\frac{da}{dN}(\max) / \frac{da}{dN}(\min) = (.98)^m / (.65)^m \quad (2)$$

One should note here that the $\frac{da}{dN}(\max) / \frac{da}{dN}(\min)$ ratio is not constant. The ratio is highly dependent on the average crack growth exponent, m. To predict the expected experimental scatter for a grouping of short fatigue crack growth curves, one needs to estimate the crack growth exponent, m, for the data. The crack growth exponent, m, is defined as the slope of the long fatigue crack growth curve directly above the bend in the curve (Table 1). The choice of m, along with equation 2, allows one to predict expected MSC growth rate data variability from the long fatigue crack growth curve (table 1). Although this simulation only considers plasticity induced closure, the expected scatter, and the procedure for obtaining the scatter, will be similar when other mechanisms of closure are introduced.

The effective stress intensity model proves to be a very powerful method to estimate upper and lower bounds on scatter in experimental MSC growth rate data. Predictions for the MSC growth rate data sets are included in table 1. For similar loading conditions (R = 0.1), the predicted $\frac{da}{dN}(\max) / \frac{da}{dN}(\min)$ ratios give good estimates of the actual scatter in the MSC growth rate experimental data. In some of the cases, the experimental scatter is higher than the predicted ratio while in others it is lower. Hence, the predictions made by Equation (2) are not to be taken as lower or upper bounds on $\frac{da}{dN}(\max) / \frac{da}{dN}(\min)$ ratios, but rather as an expected average $\frac{da}{dN}(\max) / \frac{da}{dN}(\min)$ ratio for MSC's in a given material subjected to specific loading conditions (R = 0.1). Any excess variability is caused by factors other than changes in the crystallographic orientation of the grains. For example, variability may also be caused by the interaction of cracks with microstructural barriers or with each other.

SCOPE OF THE MODEL

At this point it is important to discuss the bounds on the predictions made by the model. It is well documented that when the crack tip plastic zone spans several grains, continuum approaches work well in modeling fatigue crack growth and closure. Conversely, it has been shown here that fatigue cracks with plastic zones confined to single grains can be effectively modeled using crystal plasticity relationships. For the sake of using these variability predictions in real fatigue design problems, or to simply understand when variability may play a role in fatigue design, it is important to know where the transition from microscopic to macroscopic fatigue crack behavior occurs.

At the microscopic level, the micro-macro transition occurs when the average plastic zone size, w, is equal to the average grain size of the material, g. However, to derive a useful expression for the critical transition point, one must utilize a macroscopic variable to define the transition. This will be accomplished through the maximum applied stress intensity value, K_{max}. The average plastic zone ,w, size for a microstructurally short crack, averaged over all possible crystallographic orientations of the model, is given by the following expression (Gall et al. 1996 II):

$$w = 0.15(K_{max} / \lambda_o)^2 \quad (3)$$

where λ_o is the critical resolved shear stress of the given material. For many materials, λ_o may be approximated by half of the yield stress, $\frac{1}{2}\sigma_o$. It should be noted here that equation 3 was derived under the specific loading conditions: S_{may}/S_y = 0.6, R = 0, however, as a first approximation the concepts may be used for R = -1.0 loading conditions also. If one considers the point when the average plastic zone size reaches a value of n times the average grain size, equation 3 can be simplified to:

$$K^c_{max} = 1.29(\sigma_o)(ng)^{1/2} \quad (4)$$

where K^c_{max} is the maximum applied stress intensity value at which the critical microscopic-macroscopic transition takes place. If one applies cyclic loads with a maximum applied stress intensity below this value, then there will be inherent variability in the crack growth rate data due to grain misorientation effects. However, above this applied stress intensity value, variability in the crack growth rates caused by the microstructure will become small. By observing equation 4 it is clear that the transition is dependent on both the grain size and the yield stress of the material. If the grain size, or the yield stress are large, then crack growth rate variability will be observed at higher K_{max} values, and vice versa.

The calculated value of K^c_{max} also depends on the number of grains which needs to be spanned, n, to correctly assume continuum behavior. The value of n is not a material property, but rather a parameter which is to be chosen intuitively. The value n = 1 yields a K^c_{max} value at the point when the average crack tip plastic zone size first reaches the average grain size, and hence represents a lower bound on the scope of the growth rate variability. For example, if one considers the data of Morris and James (1983) (σ_o = 500 MPa, g = 130 μm, n = 1), K^c_{max} = 7.35 MPa $\sqrt{m}$ is obtained. If n =2 is chosen as the number of spanned grains, then K^c_{max} becomes 10.29 MPa $\sqrt{m}$. On their actual crack growth rate versus applied stress intensity plot (Fig. 9 Morris and James (1983)), the variability diminishes as 8 MPa $\sqrt{m}$ is approached, indicating that n = 1 is a reasonable choice.

CONCLUSIONS

(1) As the crystallographic orientation, ϕ, of the model was changed, the plasticity induced fatigue crack closure levels, S_{open} / S_{max}, changed dramatically. The values were found to span the range $0.02 \leq S_{open} / S_{max} \leq 0.35$.

(2) Using an average crack growth exponent read off of the long fatigue crack growth curve, along with a power law fatigue crack growth law, one can estimate experimental variations in microstructurally short fatigue crack growth rates. The experimental variations and the predicted variations matched closely (Table 1).

(3) Variability in microstructurally short fatigue crack growth rates is predicted to exist below a critical maximum applied stress intensity value, $K^c_{max} = 1.29(\sigma_o)(ng)^{1/2}$. This corresponds to a microscopic condition where the average plastic zone size is n times the average grain size, g, and

where σ_o is the yield stress of the material. From an actual data set, n = 1 gave the most reasonable results.

ACKNOWLEDGMENTS

The research is funded by the Fracture Control Program, College of Engineering, University of Illinois. Computer simulations were conducted on the SGI Power Challenge Supercomputer through grants made available by the National Center for Supercomputing Applications, University of Illinois.

REFERENCES

Asaro, Robert J. (1978) Geometrical Effects in the Inhomogeneous Deformation of Ductile Single crystals, *Acta Metallurgica*, **27**, 445-453.

Chan, K. S. (1987) Micromehanics of Small Fatigue Cracks: A Model, *Fatigue 87'*, **4**, 1802-1818.

Gall, K., Sehitoglu, H., and Kadioglu, Y. (1996 - I) F.E.M. Study of Fatigue Crack Closure Under Double Slip, *To be Published Acta. Meta.*.

Gall, K., Sehitoglu, H., and Kadioglu, Y. (1996 - II) Plastic zones and Fatigue Crack Closure Under Plane Strain Double Slip, *To be Published Met. Trans.*.

Gall, K., Sehitoglu, H., and Kadioglu, Y. (1996 - III) Predictions of Variability in Short Fatigue Crack Growth Rates, *Submitted to ASME J. Eng. Matl. Tech.* .

Larson, J.M., Williams, J.C., and Thompson, A. W. (1988) Crack Closure Effects on the growth of Small Surface Cracks in Titanium-Aluminum Alloys, *Mechanics of Fatigue Crack Closure*, ASTM STP 982, 149-167.

McClung, R. C., and Torng, T. Y. (1986) "Analysis of Small Fatigue Cracks in HSLA-80 Steel", *Fatigue 86'*, 337 - 342.

R. C. McClung and Sehitoglu, H. (1989) On the Finite Element Analysis of Fatigue Crack Closure-1. Basic Modeling Issues, *Engn. Fracture Mech.* **33**, 237-252.

R. C. McClung and Sehitoglu, H. (1989) On the Finite Element Analysis of Fatigue Crack Closure-2. Numerical Results, *Engn. Fracture Mech.* **33**, 253-272.

McEvily, A. J. and Boettner R. C. (1963) On Fatigue Crack Propagation In F.C.C Metals, *Acta Metallurgica*, **11**, 725-742.

Morris, W. L. (1977) A Comparison of Microcrack Closure Load Development for Stage I and Stage II Cracking Events for Al7075-T651, *Metallurgical Transactions A* , **8**, 1087-1093.

Morris, W., L. (1980) The Non continuum Crack Tip Deformation Behavior of Surface Microcracks, *Metallurgical Transactions A*, **11**, 1117-1123.

Morris, W. L. and James, M. R. (1983) Statistical Aspects of Fatigue Failure Due to Alloy Microstructure, *ASTM STP 811*, 179-206.

Neumann, P., (1969) Coarse Slip Model of Fatigue. *Acta Met.*, **17**, 1219.

Newman, P. and Beevers, C. J., (1986) "Growth of Short Fatigue Cracks in High Strength Ni-Base Superalloys", *Small Fatigue Cracks*, edi. R.O. Ritchie and J. Lankford, 97-116.

Pelloux, R. M. N (1969) Mechanisms of Formation of Ductile Fatigue Striations, *Transactions of the ASME*, **62**, 281-285.

Rice, J. R., Hawk, D. E., and Asaro, R. J. (1990) Crack Tip Fields in Ductile Crystals, *International Journal of Fracture*. **42**, 301-321.

Ritchie, R. O., W. Yu, D. K. Holm, A. F. Blom (1988) Development of Fatigue Crack Closure with The Extension of Long and Short Cracks in Aluminum Alloy 2124: A Comparison of Experimental and Numerical Results, *Mechanics of Fatigue Crack Closure*, ASTM STP 982, 300-316.

Sehitoglu, H. and Sun, W. (1991) Modeling of Plane Strain Fatigue Crack Closure, *J. Eng. Materials Tech.*, **113**, 31-40.

Tanaka, K., T. Hoshide, N. Sakai, (1984) Mechanics of Fatigue Crack Propagation by Crack tip Plastic Blunting, *Engineering Fracture Mechanics*, **19**, 805-825.

Tanaka, K. (1989) Mechanics and Micromechanics of Fatigue Crack Propagation, *Fracture Mechanics: Perspectives and Directions , ASTM STP 1020*. 151-183.

Taylor, D. (1988) PhD Thesis, Fatigue Crack Propagation in Nickel-Aluminum Bronze Castings, University of Cambridge, p 123.

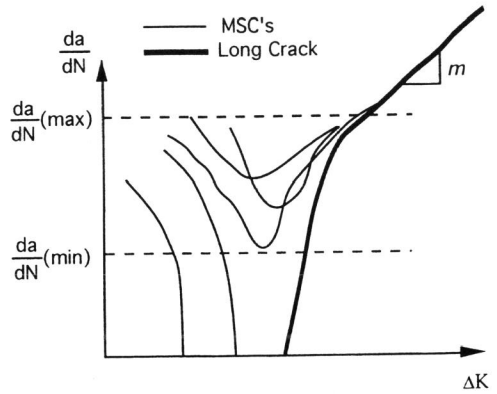

WORK [YEAR]	MATERIAL {GRAIN} {SIZE}	CRACK LENGTH RANGE	TEST CONDITIONS	$\frac{da}{dN}(\max)/\frac{da}{dN}(\min)$ experimn.	$\frac{da}{dN}(\max)/\frac{da}{dN}(\min)$ predict	m
Ritchie [1988]	2124-T351 Al {200 μm}	50 - 400 μm	R = 0.1	33	37	8.8
Newman [1986]	Nimonic 901 {230 μm}	12 - 200 μm	R = 0.1 $S_{max}/\sigma_o = .6$	30	35	8.7
Taylor [1988]	Al-Bronze {80 μm}	200 – 400 μm	R = 0.1	20	22	7.5
McClung [1989]	HSLA-80 Steel {5 μm}	2 - 12 μm	R = 0.1	16	7.5	4.9
Chan [1987]	Astroloy {50 μm}	50 – 70 μm	R = 0.1 $S_{max}/\sigma_o = .8$	11	10.4	5.7
Larson [1988]	Ti-8 Al {60 μm}	68 - 190 μm	R = 0.1 $S_{max}/\sigma_o = .6$	4	6.8	4.7

Table 1: Experimentally measured short crack growth rates in various metals. The maximum to minimum growth rate ratios are only given for cracks which eventually grow towards the long crack solution (Gall et al. 1996-III).

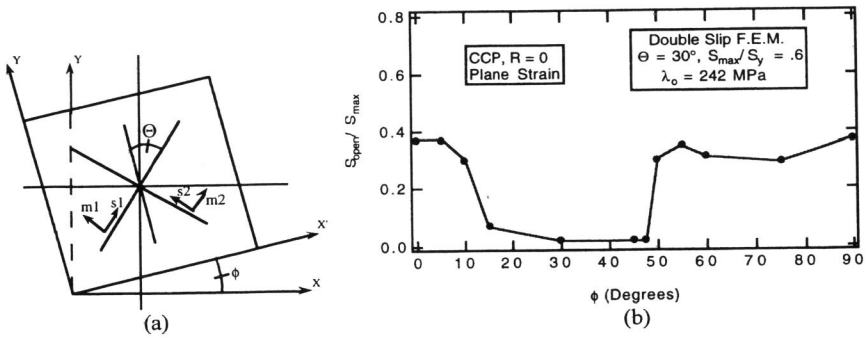

Figure 1: (a) Nomenclature used is symmetric double slip plane model. The slip directions are denoted s_1 and s_2, while the slip normals are m_1 and m_2. Rotation of the crystal is accomplished by changing ϕ, while the angle between the symmetric slip planes is varied through Θ, (b) Plot of the opening stresses versus the crystallographic orientation, ϕ, for the center cracked plate specimen. The levels are normalized by the maximum applied stresses (Gall et al. 1996-I).

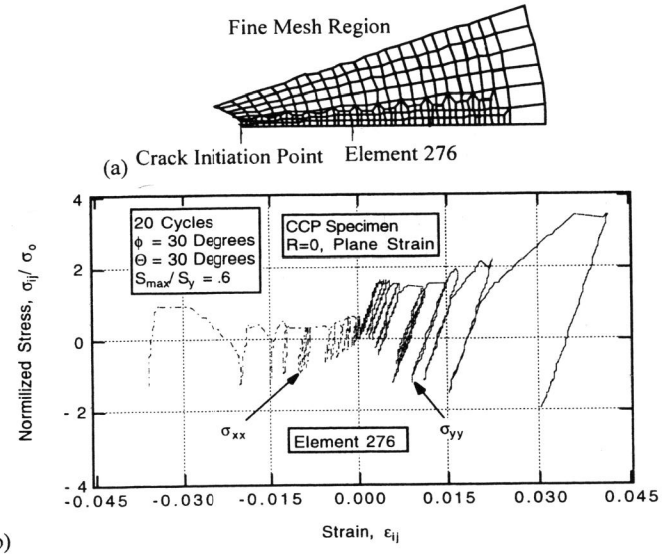

Figures 2: (a) Schematic of finite element fine mesh region demonstrating the location of the initial crack tip and Element 276. (b) Stress strain response for the crystallographic orientation ϕ = 30°. Element 276 is being approached by the crack tip, and it is located at the crack tip on the final cycle. The large hysteresis loops indicate the point where the crack tip has reached element 276.